CFD Analysis Applied to the Supersonic Research Airplane

by

Ryoji Takaki, Toshiyuki Iwamiya

National Aerospace Laboratory

and

Akiko Aoki

Sanko Software Ltd.

1 Introduction

These days research for international collaboration development of next generation High Speed Commercial Transport(HSCT) has started in order to take over the present transonic commercial transport in U.S. and Europe. As Japan is also aim to join this collaboration development, National Aerospace Laboratory (NAL) has conducted a project of an un-manned supersonic research airplane to establish design technology composed by Computational Fluid Dynamics (CFD). CFD analysis is necessary to develop HSCT which has high performance of high lift-to-drag ratio. This paper describes overview of the CFD analysis applied to the designing of the NAL's supersonic research airplane. It is necessary to validate the CFD code when the CFD is used in the designing. Therefore, the validation of CFD code is performed and results are presented in this paper.

2 Role of CFD

Figure 1 shows design cycle in the NAL project.

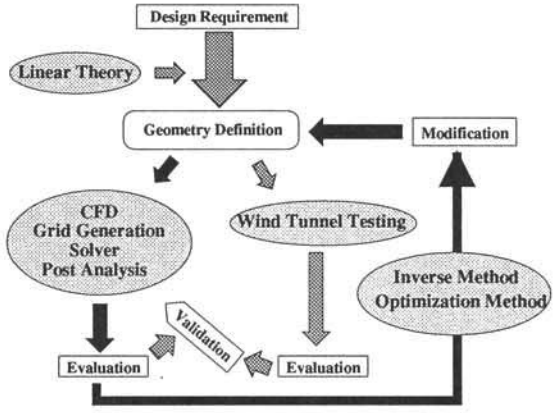

Fig. 1 Design cycle in the NAL project

First, the starting point is design requirement drew from many restrictions in each design point. The initial configuration is decided by the linear theory. CFD analysis estimates performance of this configuration. Next, the configuration is modified by inverse method [1] which is one of optimization methods. The design cycle goes round as this figure shows. Subsequently this cycle goes round over and over again and the most suitable configuration is created [2]. The role of a wind tunnel in this project is as follows; one is to obtain data for CFD validation and another is to obtain aerodynamic characteristics in off design conditions. Numerical method of CFD analysis is presented following sections.

3 Numerical methods

A flow field is regarded as a three-dimensional viscous flow with a perfect gas model. A flow on a wing surface is considered as a fully turbulent flow so that a turbulence model is used to calculate eddy viscosity.

Governing equations are discretized by a finite volume formulation. The numerical convective flux vectors are constructed by the AUSMDV scheme[3]. The MUSCL approach with TVD limiter is used in order to achieve a higher-order accuracy. The numerical viscous flux vectors are constructed by second-order central differencing scheme. Therefore, the right hand side of the discretized equations has spaciously second order accuracy.

For time integration, our code has two explicit options. One is the explicit Euler method for steady case, another is the higher-order Runge-Kutta method for unsteady case. Only steady state solutions are important in this case so that we choose the Euler explicit scheme. The convergence is accelerated by the local time stepping algorithm. Baldwin-Lomax turbulence model[4] is used on the whole surface to evaluate eddy viscosity.

In the design cycle, numerical analysis is performed to a wing-body configuration. A multi-block type structured grid system is used. Computational space is divided to fourteen blocks; six blocks in the body domain, four in the wing domain and four in the wing wake domain. The total number of grid points is about 1.4 million. This block-structured grid is generated using the multi-purpose grid generator EGG3D, developed by Dr.Takanashi[5]. Figure 2 and 3 show surface grids and outer grid, respectively. Both side of the body is presented in this figure, but actual computational space is only one side. Each block is indicated by different colors in this figure.

This document is provided by JAXA.

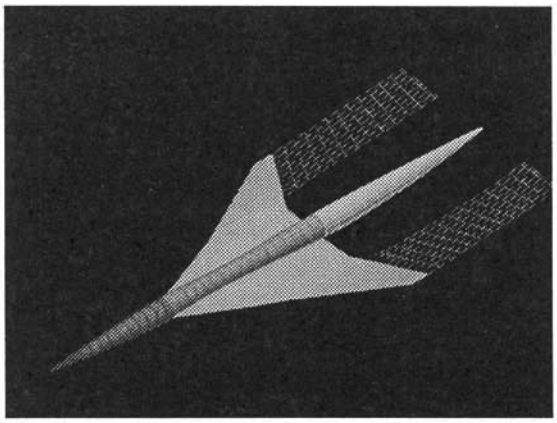

Fig. 2 Surface grid

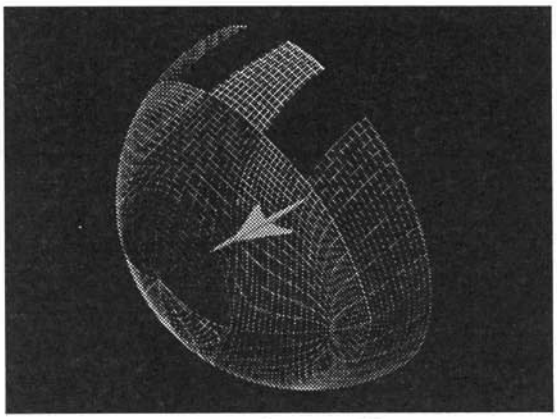

Fig. 3 Outer grid

The calculation is performed on the Numerical Wind Tunnel (NWT) at NAL. NWT is a vector parallel supercomputer with 280GFLOPS peak performance. Parallelization is performed by the domain decomposition method (DDM). Each block is assigned onto a processor of NWT. MPI and PVM message passing libraries are used in this calculation. PVM is mainly used for design calculations.

Figure 4 shows pressure distributions on first configuration of NAL's SST. The blue on the upper surface of the wing shows low pressure region and the red in the middle of the fuselage shows high pressure region.

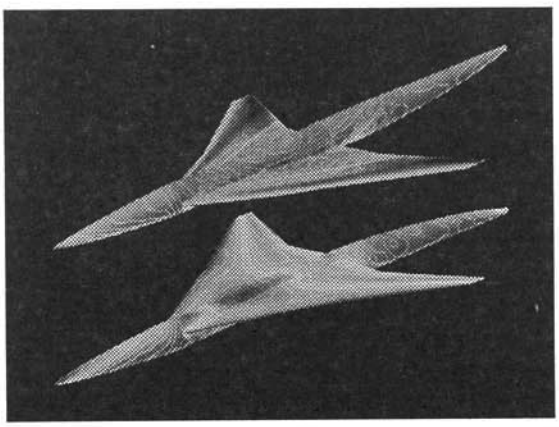

Fig. 4 Pressure distributions on NAL SST-1

Figure 5 shows pressure distributions on third configuration of NAL's SST, which is the final configuration. Regarding the final configuration, a full configuration is analyzed. So tail wings are also considered as this figure shows.

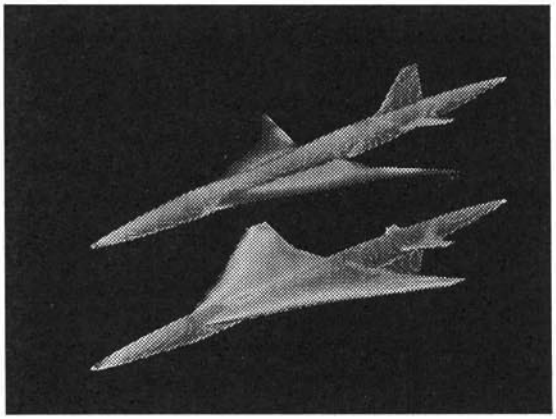

Fig. 5 Pressure distributions on NAL SST-3

4 Validations

It is important to validate the CFD code in order to establish reliability of numerical simulation. Two validation problems are performed to validate the numerical code. One is a calculation of a supersonic flow around a delta wing. Another is a calculation of a supersonic flow around a wing-body model of HSCT.

First validation problem is a supersonic flow around a delta wing [6]. Free stream mach number is 2.05 and attack angle is 4 degree. The total number of grid points is about 0.41 million and a computational space is divided into four blocks. MPI is used for parallelization. Figure 6 shows a grid system.

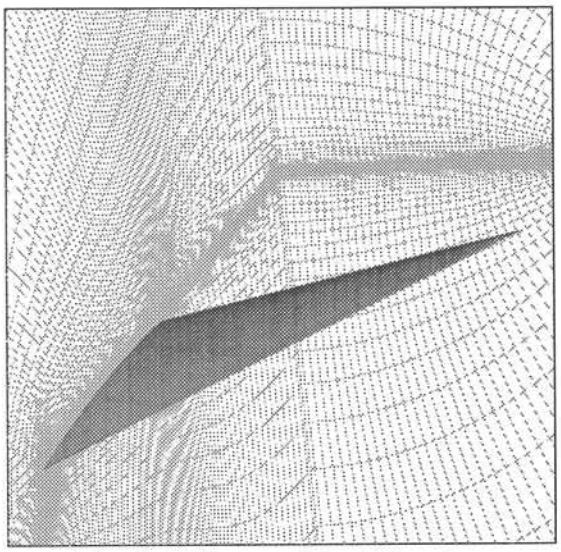

Fig. 6 Grid around the delta wing

Regarding pressure coefficient distributions at each span position of the delta wing, comparison of numerical results

This document is provided by JAXA.

and experimental data is made. Compared span positions are at 10%, 30%, 50%, 70% and 90%. Figure 7.a-e show C_p distributions at each span position. Regarding symbol, white shows numerical results and black shows experimental data. Triangle shows C_p at upper surface of the wing and square shows C_p at lower surface of the wing. It is clear that numerical results and experimental data on both surface show good agreement except the result at 90% span position. According to the other researcher's report at the workshop, this discrepancy is mainly due to deformation of the model and analysis in which deformation is considered shows a good agreement with the experimental data.

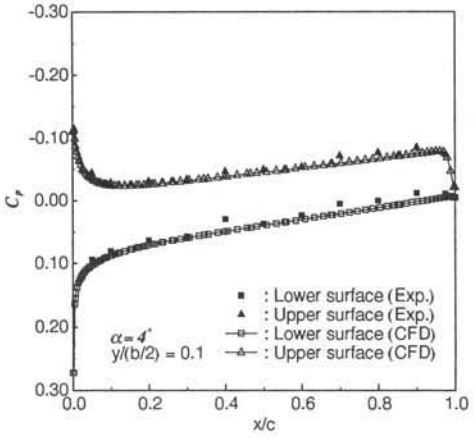

Fig. 7.a C_p distributions at 10% span position

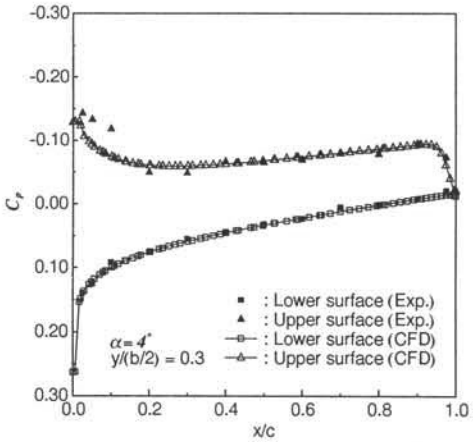

Fig. 7.b C_p distributions at 30% span position

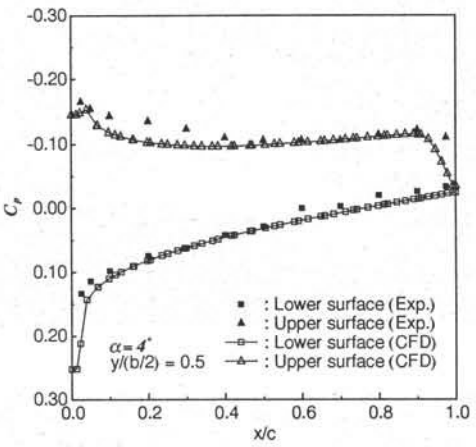

Fig. 7.c C_p distributions at 50% span position

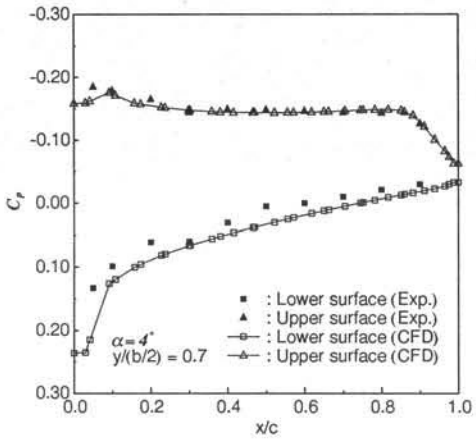

Fig. 7.d C_p distributions at 70% span position

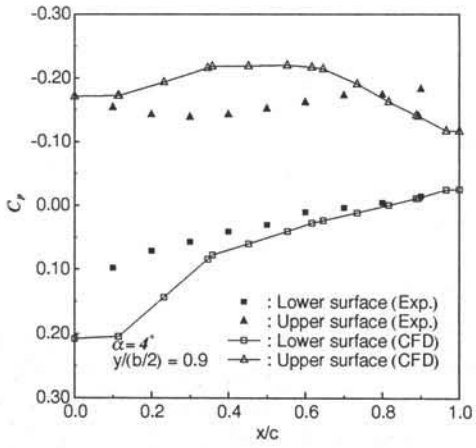

Fig. 7.e C_p distributions at 90% span position

This document is provided by JAXA.

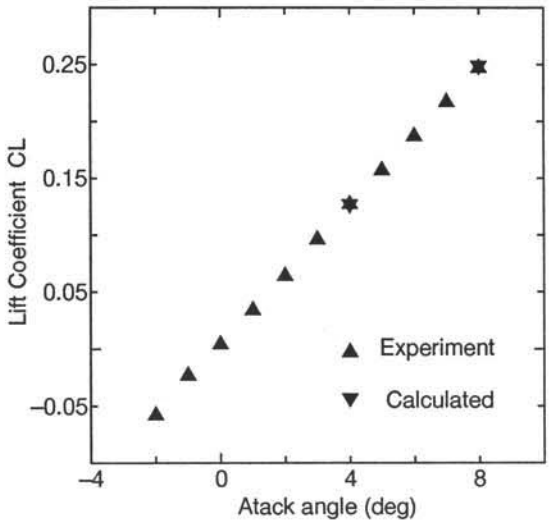

Fig. 8 attack angle vs C_L

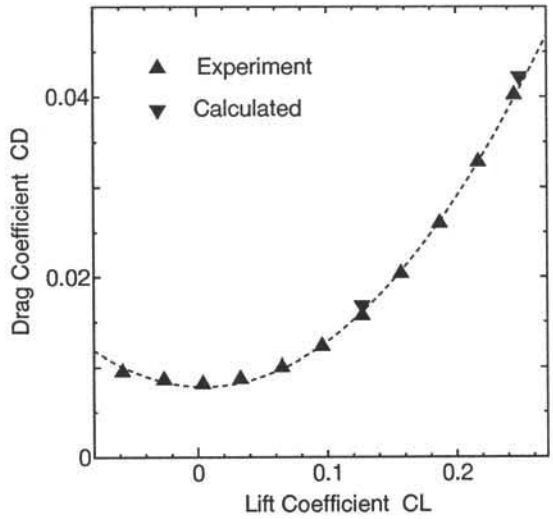

Fig. 9 C_L vs C_D

Figure 8 and 9 show characteristics of lift coefficient and drag coefficient, respectively. A result of $\alpha = 8$ degree is also plotted in these figures. Up-triangle shows experimental data. Down-triangle shows numerical results. Both figures show good agreement. They also show that the deformation of the model doesn't affect the C_L and C_D in this case.

The second validation problem is a supersonic flow around an HSCT model. This experiment was conducted at NAL. Related geometry data, experimental data and grid data will be opened at Web page at NAL. This HSCT model is a wing-body configuration. The total length is 0.85 meter and span width is 0.46 meter.

Computational space is divided into 14 blocks as same as the calculation for the design cycles of the NAL's SST, as mentioned before. The total number of grid points is about 1.15 million. MPI is used for parallelization. Free stream mach number is 2.023 and attack angle is 1.435 degree. Reynolds number is about 28 million.

Figure 10.a-d show C_p distributions at each span position. Regarding C_p distributions at 4 span positions; 13%, 50%, 77% and 93%, on the wing, a comparison between numerical results and experimental data is made. Regarding symbol, white shows numerical results and black shows experimental data. Triangle shows C_p at upper surface of the wing and square shows C_p at lower surface of the wing. It is clear that numerical results and experimental data on both surface show good agreement .

Figure 11 and 12 show characteristics of lift coefficient and drag coefficient, respectively. White symbol shows experimental data and black symbol shows numerical results. Both figures show good agreement.

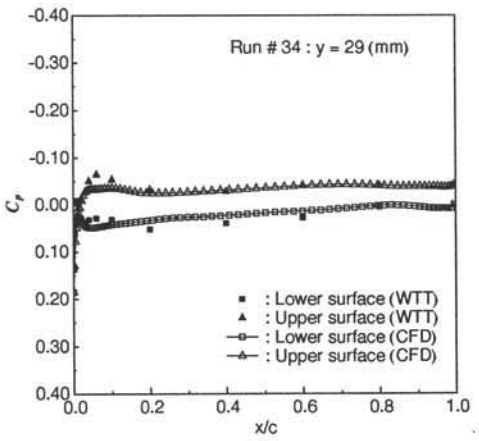

Fig. 10.a C_p distributions at 13% span position

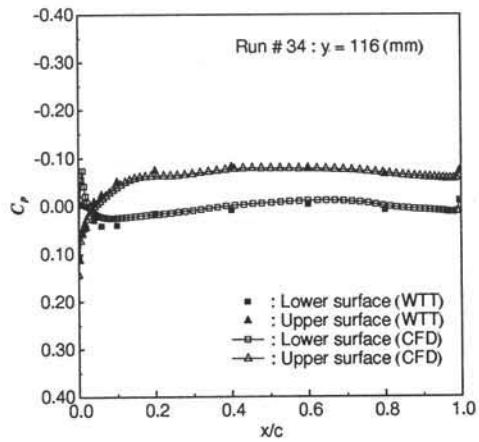

Fig. 10.b C_p distributions at 50% span position

This document is provided by JAXA.

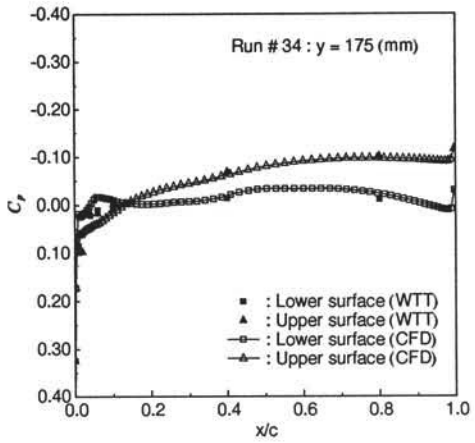

Fig. 10.c C_p distributions at 77% span position

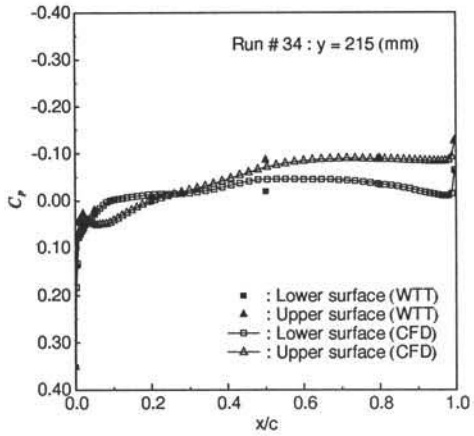

Fig. 10.d C_p distributions at 93% span position

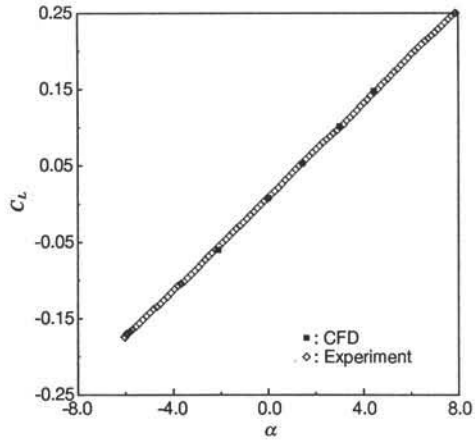

Fig. 11 attack angle vs C_L

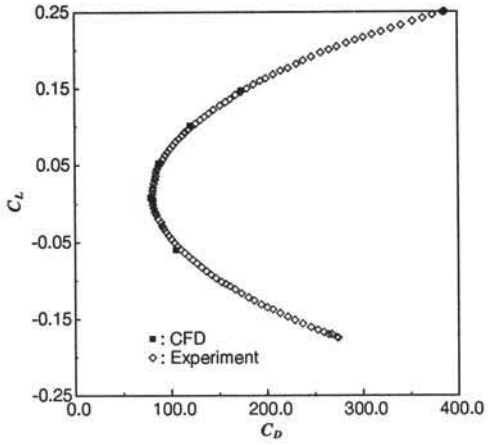

Fig. 12 C_D vs C_L

5 Conclusions

The overview and validation of numerical method applied to the design of the NAL's Supersonic Research Airplane are presented. The validation results show that CFD is an important tool to develop new generation aircraft. For future work, we will simulate a full configuration, body, wings and nacelles, of HSCT. And we are also considering combining the CFD code with a stability analysis code in order to predict a transition point.

References

[1] K. Matsushima, T. Iwamiya, S. Jeong and S. Obayashi. : Aerodynamic Wing Design for NAL's SST Using an Iterative Inverse Approach. In *1st CFD Workshop for Supersonic Transport Design*, 1998.

[2] Y. Shimbo, K. Yoshida, T. Iwamiya, R. Takaki, K. Matsushima. : Aerodynamic Design of the Scaled Supersonic Experimental Airplane. In *1st CFD Workshop for Supersonic Transport Design*, 1998.

[3] Y. Wada and M.S. Liou. : A Flux Splitting Scheme with High-Resolution and Robustness for Discontinuities. *AIAA Paper 94-0083*, 1994.

[4] B.S. Baldwin and H. Lomax. : Thin layer Approximation and Algebraic Model for Separated Turbulent Flows. *AIAA Paper 78-0257*, 1978.

[5] S. Takanashi. : Large-Scale Numerical Aerodynamic Simulations for Complete Aircraft Configurations. In *Proc. of ICAS 90, Stockholm*, 1990.

[6] R. Takaki, Y. Matsuo, T. Iwamiya and N. Hirose. : First Europe-US High Speed Flow Field Database Workshop Part II. 1997.

This document is provided by JAXA.